



## Geochemical techniques to discover open cave passage in karst spring systems



Elizabeth A. Hasenmueller\*, Robert E. Criss

Department of Earth and Planetary Sciences, Washington University, Campus Box 1169, 1 Brookings Drive, Saint Louis, MO 63130-4899, USA

### ARTICLE INFO

#### Article history:

Received 16 March 2012

Accepted 16 November 2012

Available online 4 December 2012

Editorial handling by R.B. Wanty

### ABSTRACT

Dissolved O<sub>2</sub> (DO) and pH data provide a novel, inexpensive field method to detect open cave passages in karst spring systems that can be complemented by laboratory measurements of major elements and nutrients, total suspended solids (TSS), *Escherichia coli* (*E. coli*) levels, and stable isotopes. Karst springs in east-central Missouri that have no known air-filled passages (“phreatic” springs) typically have low DO and pH values (<80% saturation and <7.7, respectively), which are characteristic of groundwaters that do not communicate with the atmosphere. In contrast, springs draining vadose cave passages have higher DO and pH values (>60% saturation and >7.7, respectively) that resemble surface waters due to the equilibration of DO with the overlying cave atmosphere and the simultaneous degassing of dissolved CO<sub>2</sub>. Traverses down phreatic spring branches show exchange with the atmosphere causes an increase in DO only a short distance downstream of the spring orifice, while the pH concurrently increases due to the degassing of CO<sub>2</sub>. Further downstream both parameters tend to level off reflecting a general approach to equilibrium under surface conditions, though this process is more rapid for DO than for pH. In contrast, the DO and pH along cave spring branches change little from values at the cave entrance. Additionally, (1) degassing processes affect the saturation state of calcite, with cave springs being the most saturated with respect to calcite, (2) phreatic springs typically have lower TSS and *E. coli* levels than open cave springs due to slower and less variable flow delivery, longer residence times, and less turbulent flow, and (3) phreatic springs tend to plot on the global meteoric water line (MWL), while waters from open cave systems tend to be enriched in <sup>18</sup>O and D and can plot below the line due to evaporation and exchange of the water with the overlying cave atmosphere.

© 2012 Elsevier Ltd. All rights reserved.

### 1. Introduction

Discovery and exploration of underground passages are important for ecosystem conservation, to delineate their potential as collapse hazards, and to identify subsurface avenues for the transport of shallow groundwater and its pollutants. Unfortunately, statistical methods show that most caves remain undiscovered as they lack large openings (e.g., White, 2005; Criss et al., 2006). Any systematic method for cave discovery must involve familiarity with the geologic framework essential to cave formation. For example, knowledge of stratigraphic contact locations is crucial, because where insoluble rock overlies soluble rock there is an elevated potential for formation of solution caves (Ford, 1971; Palmer, 1975). Karst topography including the presence of sinkholes, losing streams, and springs commonly indicates the presence of underlying cave passages, but caves may be present when such features are mantled or absent.

Less conventional methods, such as air movement through openings at the ground surface, have also been used to detect

caves. Wind Cave, Jewel Cave, and Lechuguilla Cave were all discovered by investigating air drafts on the surface that are generated as subsurface voids respond to changes in atmospheric pressure (Palmer, 2007). On cold winter days, such air flow can cause visible condensation clouds above cave entrances, an effect that led to the historical discovery of Valentine Cave in northeastern California. Infrared mapping has also facilitated cave discovery by exploiting the temperature contrast between the relatively warm cave exhalations and the ambient air (Brown, 1972; Campbell et al., 1996; Thompson and Marvin, 2005).

Geophysical techniques are often employed to locate and map subsurface passages. Gravity surveys (Smith and Smith, 1987), electrical resistivity (Noel and Xu, 1992), natural potential surveys (Lange, 1999), ground-penetrating radar (Murphy et al., 2005), seismic surveys (Cook, 1965), and other methods (Stierman, 2004) have all been employed to detect karstic voids. Nevertheless, these methods have differing sensitivities that vary with subsurface conditions, and none provide a “magic bullet” for cave prospecting (Bechtel et al., 2007).

This paper shows that geochemical measurements provide a valuable, complementary method to detect open cave passage in carbonate-hosted spring systems. In particular, DO and pH

\* Corresponding author. Tel.: +1 314 935 7475; fax: +1 314 935 7361.

E-mail address: [eahasem@wustl.edu](mailto:eahasem@wustl.edu) (E.A. Hasenmueller).

measurements can be effectively used in the field, and these data can be augmented by laboratory measurements of major elements and nutrients (used for geochemical calculations), TSS, *E.coli* levels, and stable isotopes.

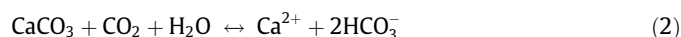
## 2. Basis for geochemical cave detection

Recharge and subsurface waters are depleted in O<sub>2</sub> and enriched in CO<sub>2</sub> due to respiration and decomposition processes, but re-equilibrate to near-surface or surface values when they contact open air, either inside a cave or above ground (Palmer, 2007). The degassing of CO<sub>2</sub> when saturated groundwaters encounter open air is well established (Ek and Gewalt, 1985; Drever, 1997; Langmuir, 1997; Baldini et al., 2006), and the depletion of DO in recharge waters has also been observed (Jacobson and Langmuir, 1974; Boulding and Ginn, 2004). Thus, DO and pH values respond to vadose passages in carbonate-hosted caves, suggesting that field meters can be used at spring orifices to elucidate whether the upstream passages are open or closed.

This method is centered on the basic biochemical processes of O<sub>2</sub> removal and CO<sub>2</sub> production by respiration, and the reverse by photosynthesis:



as well as the abiotic process of calcite dissolution and precipitation in carbonate-hosted springs:



Of course many other processes, such as those involving chemical oxygen demand, can also play a role in the relative gas contents of spring water.

The pH of pure water in equilibrium with the atmosphere ( $P_{\text{CO}_2} = 10^{-3.5}$  bar) is 5.66 and is representative of unpolluted rain water, but if calcite is present, the pH of an equilibrated, open aqueous system is 8.26 (i.e., carbonate-hosted waters). However, dissolved CO<sub>2</sub> concentrations in limestone aquifers are almost always above values expected for waters in equilibrium with the atmosphere (Holland et al., 1964; Back and Hanshaw, 1970; Langmuir, 1971). This is a consequence of the high CO<sub>2</sub> concentration (typically  $10^{-2.5}$ – $10^{-1.5}$  bar) in the soil atmosphere (Troester and White, 1984; White, 1988), that is a result of microbial and plant root respiration, decay of organic matter, and the restricted circulation of soil air. Moreover, O<sub>2</sub> is often 5–20% of the soil atmosphere ( $10^{-1.3}$ – $10^{-0.7}$  bar), but can drop to almost zero in poorly drained soils (Patrick, 1977; Brady and Weil, 2008). Thus, as rain percolates through the soil, CO<sub>2</sub> typically increases to an equivalent fugacity ( $f_{\text{CO}_2}$ ) of  $10^{-2}$  bar in soils of humid, temperate areas (Langmuir, 1997) while  $f_{\text{O}_2}$  concomitantly decreases. These high CO<sub>2</sub>, low O<sub>2</sub> soil waters then recharge local aquifers, where organic matter decay can continue.

The CO<sub>2</sub>-rich soil and recharge waters are largely responsible for the high contents of total dissolved CO<sub>2</sub> in subsurface water. If closed system waters flow to an open system, such as an air-filled cave passage or a spring orifice, they degas their high CO<sub>2</sub> contents and take up O<sub>2</sub> to achieve equilibrium with the lower  $P_{\text{CO}_2}$  and higher  $P_{\text{O}_2}$  of the overlying air. This re-equilibration commonly leads to calcite deposition, sometimes evidenced by the development of speleothems (Dreybrodt, 2005), and can lead to dramatic increases in pH. This process has been observed in groundwater seeps in Paulter Cave, Illinois, which generally had a lower pH than water in the cave streams (Friedrich et al., 2011). Not all recharge is through soil (e.g., recharge by sinking streams and “naked karst,” including limestone outcrops and karren fields), however, the springs in this study are largely recharged through soils.

## 3. Regional hydrologic setting and study sites

East-central Missouri (Fig. 1) is ideal for a cave detection study because of the diverse karst terrain. This densely vegetated region has abundant rainfall (~100 cm/yr) and rugged topography (Vandike, 1995), and is predominantly underlain by Paleozoic limestone and dolostone units that dip away from the St. Francois Mountains (Fenneman, 1938). This combination of factors promotes interactions between soluble carbonate rocks and flowing groundwaters that are undersaturated with respect to calcite, and has led to the extensive development of karst features including abundant sinkholes, caves, springs, seeps, and losing and gaining streams (Criss et al., 2009). In particular, the region shown in Fig. 1 includes thousands of sinkholes, more than 500 caves, and several hundred springs including the first-magnitude Maramec Spring (e.g., Vineyard and Feder, 1982).

Mississippian and Ordovician limestones host the majority of the features studied here, though one watershed is underlain by Ordovician St. Peter Sandstone and one spring issues from Quaternary alluvium. Most features are located in sinkhole plains or in their highly modified, urban remnants (Vineyard and Feder, 1982; Criss et al., 2006), and several mapped caves of varying size were included in the study: Babler Cave, Cliff Cave, Double Drop Cave, and Onondaga Cave (Fig. 1; for cave maps see Baker and Streamer, 2002; maps SLO-004, SLO-013, SLO-065, and CRD-001, respectively).

## 4. Materials and methods

### 4.1. Samples

Water samples representing a broad range of catchment size and land development (e.g., urban, agricultural, and forested) were collected, mostly under normal flow conditions. A total of 46 features including phreatic springs, cave springs, resurgences, surface streams, wastewater treatment plant (WWTP) effluents, and a lake (Fig. 1) were sampled on multiple occasions to document variations in DO and pH. Extensive chemical datasets were assembled over a 2-year period (2010–2011), and further contributions were made to a series of field and isotope measurements that have been maintained for the last 16 years for numerous phreatic springs and cave springs. Samples were collected throughout the year, but most were obtained during the summer when soil respiration effects are largest. The only springs that were sampled during a storm event were Kiefer Spring and Rockwoods Spring, and these two samples are labeled on all the relevant figures. All other samples, including additional samples of Kiefer Spring and Rockwoods Spring, were collected 3–14 days after rainfall. Details of sample dates and basin conditions are presented in extensive tables by Hasenmueller (2011).

In the following, the term “phreatic” spring is applied to features that lack known cave passage, although there is the possibility that undiscovered, air-filled passages exist. In contrast, the term “cave” spring is used to describe streams issuing from enterable caves. Only perennial, flowing phreatic springs and cave springs were selected; mean discharges ranged from 0.0001 to 4.1 m<sup>3</sup>/s, which equates to effective catchment areas of <10–450 km<sup>2</sup> (Vineyard and Feder, 1982).

### 4.2. Chemical analyses

Water chemistry analyses for each feature consisted of field measurements of DO, pH, temperature, specific conductivity (SpC), and turbidity, as well as laboratory analyses of major elements and nutrients, TSS, coliform bacteria, and O and H isotopes.

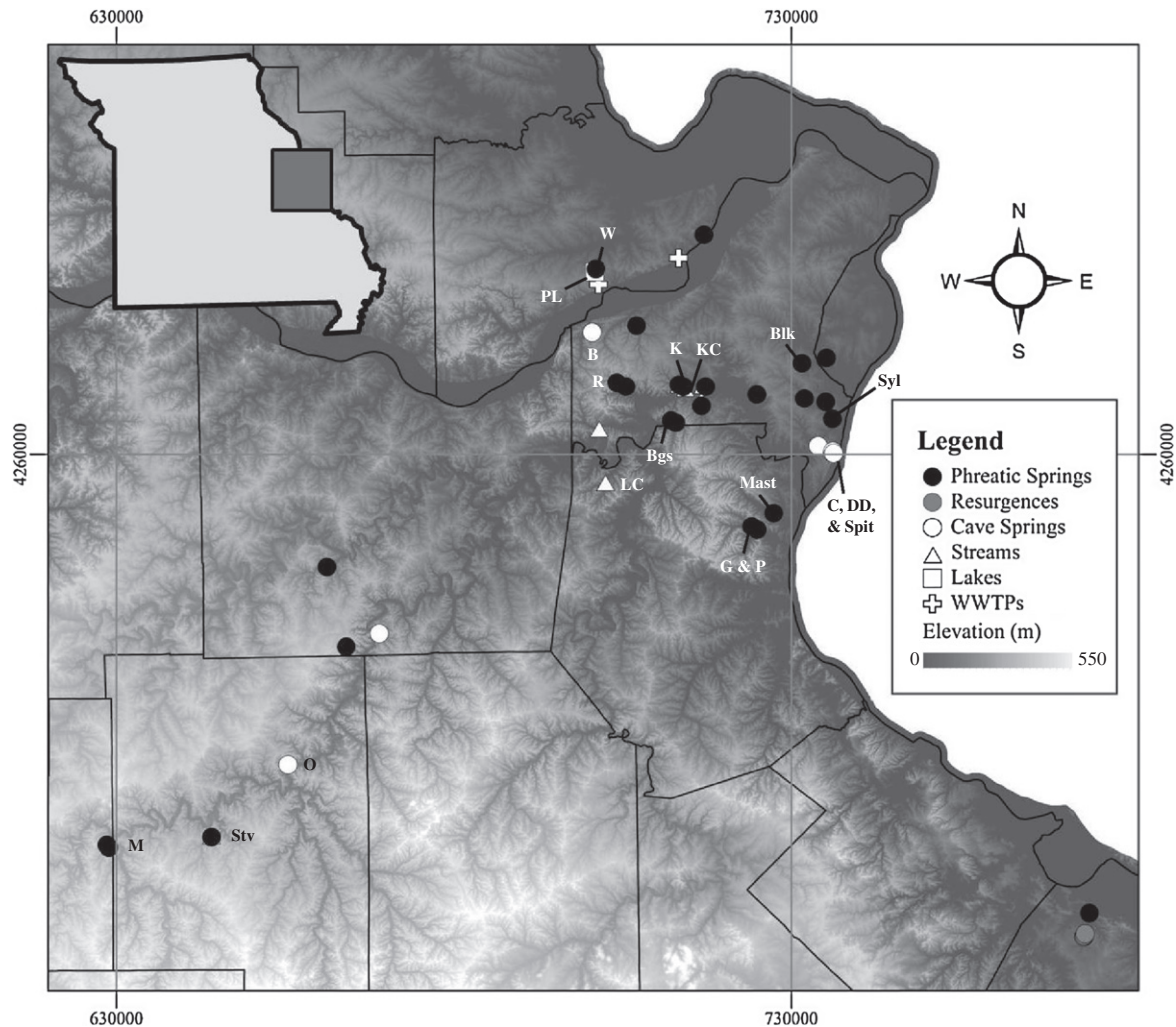


**Fig. 1.** Relief map of east-central Missouri showing sample locations. The elevation ranges from 390 m in the SW to 110 m along the Mississippi River in the SE. Selected cave springs (Babler Cave, B; Cliff Cave, C; Double Drop Cave, DD; Onondaga Cave, O; and Spit Cave, Spit), phreatic springs (Blackburn, Blk; Bluegrass, Bgs; Glatt's, G; Kiefer, K; Maramec, M; Mastodon, Mast; Pevely Milkhouse, P; Rockwoods, R; Steelville, Stv; Sylvan, Syl; and Weldon, W), surface streams Kiefer Creek (KC) and LaBarque Creek (LC), and Prairie Lake (PL) are labeled. Due to the scale of the map, feature symbols overlap in several locations. Digital elevation model (DEM) basemap data are generated using U.S. Geological Survey (USGS) data and are provided by Missouri Spatial Data Information Service (MSDIS, 2011); overlain on the DEM are the county lines from the 2010 U.S. Census and are provided by MSDIS (2011). Gridlines are in UTM eastings and northings (Zone 15, NAD 83).

Field DO measurements were made in both mg/L and % saturation; however, % saturation was used for comparison between features because overall dissolved  $O_2$  concentration depends on temperature, air pressure, and salinity. Following geochemical convention, % saturation refers to the comparison of the measured DO concentration to the concentration that would theoretically exist at equilibrium at the measured water conditions. Measurements at the orifice were made for all springs. Multiple traverses along several spring branches were also carried out to identify dynamic changes in water chemistry downstream of the orifice. These traverses were selected based on the length of the spring branch. Short spring branches, including those that extend only a few meters before joining a surface stream or returning to the subsurface via a swallow hole, or those artificially dammed near the orifice, were not selected for traverse studies. Traverses within the caves were not possible due to the limited access to these features as a measure to curtail the spread of white nose syndrome in bats. Measurements at the spring orifice were repeated at the end of each series to determine if any instrumental drift occurred during the sampling interval; these duplicate measurements consistently showed minimal drift. In particular, the DO varied less than

0.2 mg/L and 1.5%, pH varied less than 0.02 units, and SpC varied less than 0.3%, all within error of the instruments ( $\pm 0.3$  mg/L or 2% of reading, 0.02 pH units, and 0.5% of the reading, respectively).

The elemental composition of field-acidified and field-filtered water samples was measured using a Perkin-Elmer Optima 7300DV inductively-coupled plasma optical emission spectrometer (ICP-OES) in accordance with the techniques outlined in U.S. Environmental Protection Agency (USEPA) Method 200.7 (USEPA, 1990). Instrument operation and data processing were performed with WinLab32™ software. Blanks, reference standards (Trace-CERT®, Sigma-Aldrich), and duplicate and triplicate samples were run with each sample set to check the precision and accuracy of analytical procedures; laboratory accuracy was  $\pm 5\%$ . Detection limits for relevant elements are listed in Table 1.

Subsamples for major ions, including  $Cl^-$ ,  $NH_4^+-N$ ,  $NO_3^- -N$ , and total P as  $PO_4^{3-}$ , were collected in either pre-cleaned high density polyethylene (HDPE; i.e.,  $Cl^-$ ,  $NH_4^+-N$ , and  $NO_3^- -N$ ) or glass (i.e., total P) bottles. Samples for TSS and coliform bacteria determination were also collected in HDPE bottles, and all coliform bacteria sample bottles were autoclaved. The  $Cl^-$ ,  $NH_4^+-N$ ,  $NO_3^- -N$ , total P, TSS, and coliform bacteria analyses were determined using



**Table 1**  
Concentration means and ranges for selected water quality constituents for various types of waters<sup>a</sup>.

	Phreatic springs	Resurgences	Cave springs	Streams	Treated wastewater	Lake
Total sampling sites	25	4	7	7	2	1
Temperature (°C) ± 0.1 °C	14.7	15.3	14.5	16.8	17.9	35.0
	12.5–19.4	14.6–15.8	11.9–16.9	14.3–20.1	14.4–24.6	
SpC (µS/cm) ± 0.5%	760	613	809	515	797	104
	261–1524	595–624	481–1014	191–805	773–822	
DO (% saturation) ± 2%	53.9	77.0	76.9	60.7	88.5	80.1
	11.5–84.6	72.0–86.5	60.1–98.5	43.3–84.1	66.4–107.8	
DO (mg/L) ± 0.3 mg/L	5.50	7.62	7.87	5.96	8.54	5.44
	1.23–8.72	7.01–8.58	6.08–10.16	4.02–8.21	5.53–10.92	
pH ± 0.02 units	7.35	7.69	7.95	7.88	8.15	9.66
	6.93–8.13	7.65–7.72	7.70–8.18	7.62–8.07	8.00–8.30	
TSS (mg/L) ± 1 mg/L	22	–	52	92	23	–
	1–225	–	6–126	1–598	10–35	
<i>E. coli</i> (cfu/100 mL) <sup>b</sup>	– <sup>c</sup>	33	– <sup>c</sup>	– <sup>c</sup>	687	14
	6->2420	0–100	15->2420	31->2420	3–1986	
δ <sup>18</sup> O (‰) ± 0.1‰	–6.7	–5.2	–6.5	–6.2	–8.4	–3.2
	–8.0 to –3.4	–5.2 to –5.2	–7.3 to –5.7	–6.8 to –5.5	–9.3 to –7.2	
δD (‰) ± 1‰	–43	–34	–43	–41	–57	–30
	–58 to –18	–33 to –34	–49 to –40	–46 to –35	–62 to –50	
Carbonate alkalinity (mg/L) <sup>d</sup>	269	227	278	214	154	23
	107–442	224–232	216–320	65–317	110–203	
Ca <sup>2+</sup> (mg/L) ± 0.01 mg/L	95.5	59.4	100.0	67.5	53.3	9.6
	32.6–163.5	59.0–59.9	75.2–125.7	21.0–103.6	46.1–65.3	
Mg <sup>2+</sup> (mg/L) ± 0.01 mg/L	16.7	24.4	19.9	12.5	17.0	2.0
	6.5–34.2	23.3–25.1	13.4–31.6	3.4–16.6	16.0–18.2	
HCO <sub>3</sub> <sup>–</sup> (mg/L) <sup>d</sup>	384	290	351	285	190	23
	160–744	287–296	269–410	101–434	135–253	
log <i>f</i> CO <sub>2</sub> (bar) <sup>d</sup>	–1.93	–2.33	–2.46	–2.58	–2.96	–5.35
	–2.82 to –1.31	–2.36 to –2.29	–2.72 to –1.97	–2.98 to –2.27	–3.13 to –2.69	
log <i>f</i> O <sub>2</sub> (bar) <sup>d</sup>	–1.02	–0.82	–0.82	–0.95	–0.77	–0.82
	–1.62 to –0.72	–0.86 to –0.77	–0.96 to –0.71	–1.07 to –0.90	–0.89 to –0.67	

<sup>a</sup> Accuracy specified by manufacturer or detection limit for elements measured on ICP-OES reported as the concentration corresponding to a signal three times the noise of the background.

<sup>b</sup> Most probable number range: <1–2420 cfu/100 mL.

<sup>c</sup> Obtaining an average was not possible due to off-scale measurements.

<sup>d</sup> Calculated using Geochemist's Workbench Standard 8.0.

USEPA-approved techniques (Hach, 2005a,b,c,d,e; USEPA, 1971, respectively).

Subsamples for O and H isotopic analyses were collected in clean, air-tight glass bottles. Isotopic measurements of untreated water samples were made with an automatic Thermo Finnigan MAT 252 ion ratio mass spectrometer (IR-MS) with a peripheral PAL device. The data are reported in the conventional manner, as δ<sup>18</sup>O and δD values that represent ‰ deviations from standard mean ocean water (V-SMOW). The δ<sup>18</sup>O values of sample waters were determined by equilibrating 0.5 mL of the water sample with a 0.3% CO<sub>2</sub>/He gas mixture at 1 bar for 16–24 h at 26.5 °C and analyzing the CO<sub>2</sub> gas; precision is ±0.1‰. The δD values were determined by reacting 1.0 µL of water with metallic Cr at 800 °C to produce H<sub>2</sub> gas prior to analysis; precision is ±1.0‰. Every run included several standards and duplicates and triplicates of samples to check the precision and accuracy of analytical procedures.

#### 4.3. Geochemical modeling

Concentrations of HCO<sub>3</sub><sup>–</sup> were calculated using ion balancing for the measured major ions (including the cations: Ca<sup>2+</sup>, K<sup>+</sup>, Mg<sup>2+</sup>, Na<sup>+</sup>, and NH<sub>4</sub><sup>+</sup>–N and the anions: Cl<sup>–</sup>, NO<sub>3</sub><sup>–</sup>–N, PO<sub>4</sub><sup>3–</sup>, SiO<sub>4</sub><sup>4–</sup>–Si, and SO<sub>4</sub><sup>2–</sup>–S) and pH. The *f*O<sub>2</sub>, *f*CO<sub>2</sub>, and carbonate alkalinity values were calculated using Geochemist's Workbench<sup>®</sup> Standard 8.0 react applet using HCO<sub>3</sub><sup>–</sup> as the charge balancing anion.

## 5. Results

The results of the spring survey are discussed in the following subsections. Relevant chemical data for the features are summa-

rized in Table 1. Detailed tables of data for individual sampling locations are provided in Hasenmueller (2011).

### 5.1. Dissolved oxygen and pH

The DO and pH values plotted in Fig. 2 show distinct differences between phreatic springs and cave springs. For the aforementioned reasons, gas equilibration in open cave systems results in systemically higher DO and pH in passage waters. However, due to different chemistries among the recharge waters and their subsequent subsurface paths, and because some of the “phreatic” springs may be incorrectly classified, there is a continuum of DO and pH values with some overlap (gray bar, Fig. 2).

#### 5.1.1. Rate of degassing

Traverses down the branches of both types of springs establish how gas equilibration processes affect these waters (Fig. 3). These equilibration rates are comparable to the surface exposure time for these features, and, thus, both kinetic and equilibrium concepts apply; that is, gas solution–exsolution reaction rates typically have half-times on the order of minutes (Langmuir and Mahoney, 1985), which is consistent with channel velocity and length. Therefore, progressive degassing and equilibrium processes were observed along all the phreatic spring traverses.

Equilibration of pH was typically slower than for DO, a phenomenon that has been observed in other carbonate springs (Omelon et al., 2006), and most springs did not reach steady pH values by the end of the traverse (Fig. 4). On the other hand, DO equilibration was quite rapid for the springs; typically, steady state was attained in the first 150 m of the traverse. Phreatic springs showed large

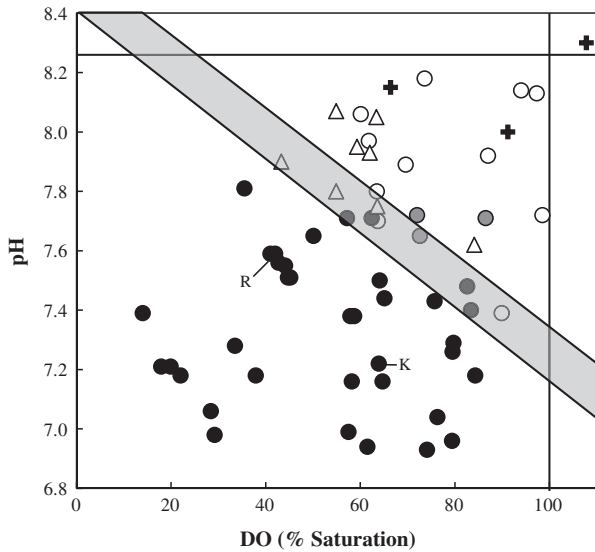


**Fig. 2.** The pH versus DO (% saturation) for phreatic springs (closed circles), cave springs (open circles), resurgences (gray circles), surface streams (open triangles), and treated wastewater (crosses); all spring samples shown were measured at the orifice. Lines for DO saturation (100%) and the pH of pure water in equilibrium with the atmosphere and calcite (8.26) are plotted for reference. Prairie Lake is off-scale with a pH of 9.66 and DO of 80%, and one wastewater sample was supersaturated (DO > 100%), likely due to aeration processes during treatment. Specific samples collected during a storm event for Kiefer Spring (K) and Rockwoods Spring (R) are also shown. Note the minor overlap (gray bar) of the fields for phreatic springs and cave springs.

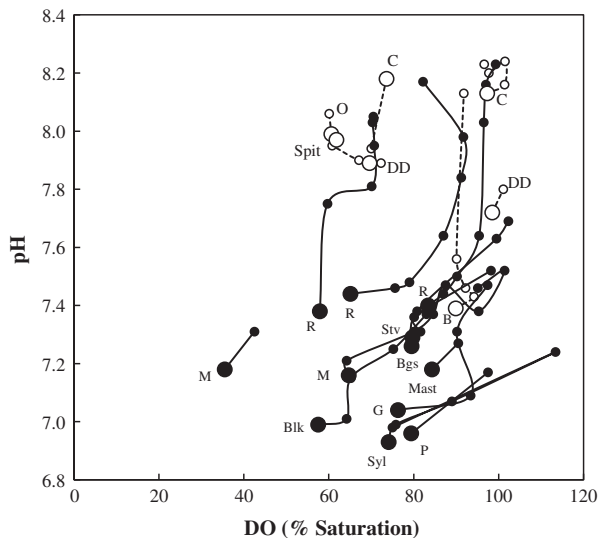


**Fig. 3.** The pH versus DO (% saturation) for phreatic springs (closed circles and solid lines) and cave springs (open circles and dashed lines) along traverses. Measurements made at spring orifices (large circles) and along spring branches (small circles) are shown. Phreatic springs exhibit large increases in DO and pH to reach equilibrium with the atmosphere; cave springs, however, generally increase very little, maintaining their DO and pH values, or even decreasing somewhat due to biological activity. All cave springs (Babler Cave, B; Cliff Cave, C; Double Drop Cave, DD; Onondaga Cave, O; and Spitt Cave, Spitt) and phreatic springs (Blackburn, Blk; Bluegrass, Bgs; Rockwoods, R; Glatt's, G; Maramec, M; Mastodon, Mast; Pevely Milkhouse, P; Steelville, Stv; and Sylvan, Syl) where traverses were made are labeled. Distances between sampling locations along the traverses are shown in Fig. 4.

increases in pH, sometimes by almost a pH unit, and similar behavior has been observed in other carbonate-hosted springs (Uzdowski et al., 1979; Dandurand et al., 1981). In contrast, cave springs gen-

erally showed only small increases in pH of less than 3% that occurred within the first 30 m of the traverse, with the exception of Babler Cave Spring (Fig. 1). Concomitant decreases in DO of >10% usually occurred, presumably due to microbial activity. Small cave systems, such as Babler Cave Spring, which has a length of only 30 m and maximum passage diameter of 3 m (Baker and Streamer, 2002; map SLO-004), had lower DO and pH and varied more along a traverse down its spring branch. This is likely a result of the small atmospheric volume with which the cave stream can equilibrate.

These equilibration processes can be approximated by the equation:

$$(C - C_{eq}) / (C_i - C_{eq}) = e^{-kd} \quad (3)$$

where  $C$  is the concentration at a given distance,  $C_i$  is the orifice concentration,  $d$  is the distance from the orifice which is a proxy for time, and  $k$  is a constant. However, the final equilibrium concentrations are not precisely known and can be unique for each feature because multiple and complex processes affect the equilibrium endpoint (Dandurand et al., 1981). Consequently, one cannot assume that these features equilibrate completely with the atmosphere by the end of the traverses.

### 5.1.2. Effects of nutrients

Springs that have high nutrient loads (typically  $\text{NH}_4^+ - \text{N} > 0.2$  mg/L and  $\text{PO}_4^{3-} > 0.5$  mg/L; e.g., urban Blackburn Spring; Fig. 1) have low DO and pH at the orifice (<60% saturation and <7.0, respectively; Figs. 3 and 4) due to enhanced biological activity. However, there were no discernible trends between DO and pH and  $\text{NO}_3^- - \text{N}$  concentrations for the springs. The most dramatic expression of high nutrient availability was noticed several meters away from the Sylvan Spring orifice (Fig. 1), where more light was available and large algal mats were evolving visible gas bubbles, presumably via photosynthetic  $\text{O}_2$  production. This effect is minimal at the spring orifices where cool waters emerge from the dark subsurface or where spring branches are heavily shaded, as both of these conditions are less conducive to photosynthetic activity.

### 5.2. Calcite saturation

Additional chemical analyses and modeling document the influence of  $\text{CO}_2$  degassing on the saturation state of carbonate minerals in the phreatic springs and cave springs. Here it is useful to employ the saturation index,  $SI$ , defined as the  $\log_{10}(Q/K)$ , where the reaction quotient,  $Q$ , is compared to the equilibrium constant,  $K$  (Langmuir, 1997). For saturated systems,  $SI = 0$ , whereas  $SI < 0$  if undersaturated and  $SI > 0$  if oversaturated.

In Fig. 5 the relationship between  $\text{Ca}^{2+}$  and  $f\text{CO}_2$  contents and calcite saturation are shown as defined by  $SI$ . Cave spring waters are typically supersaturated with respect to calcite, and their  $SI$ s are typically greater than 0.5, but can exceed 1.2, while phreatic springs have  $SI$ s under 0.5 and are commonly undersaturated (Fig. 5). Supersaturation in both types of spring water is, in part, attributed to elevated concentrations of dissolved carbonate species in recharge area soil waters, but in cave systems is also a result of  $\text{CO}_2$  degassing that leaves the  $\text{Ca}^{2+}$  concentration unchanged until precipitation of calcite occurs. However, the cave air was not always fully equilibrated with the surface air, and evidence of further degassing was observed at a waterfall below Double Drop Spring (Fig. 1), where tufa deposition occurs. Another minor effect on these cave waters is evaporation, which increases the  $\text{Ca}^{2+}$  concentration. These evaporation and degassing processes are key driving forces in the formation of speleothems (Baldini et al., 2008), as confirmed by stable isotope data (see Section 5.4).

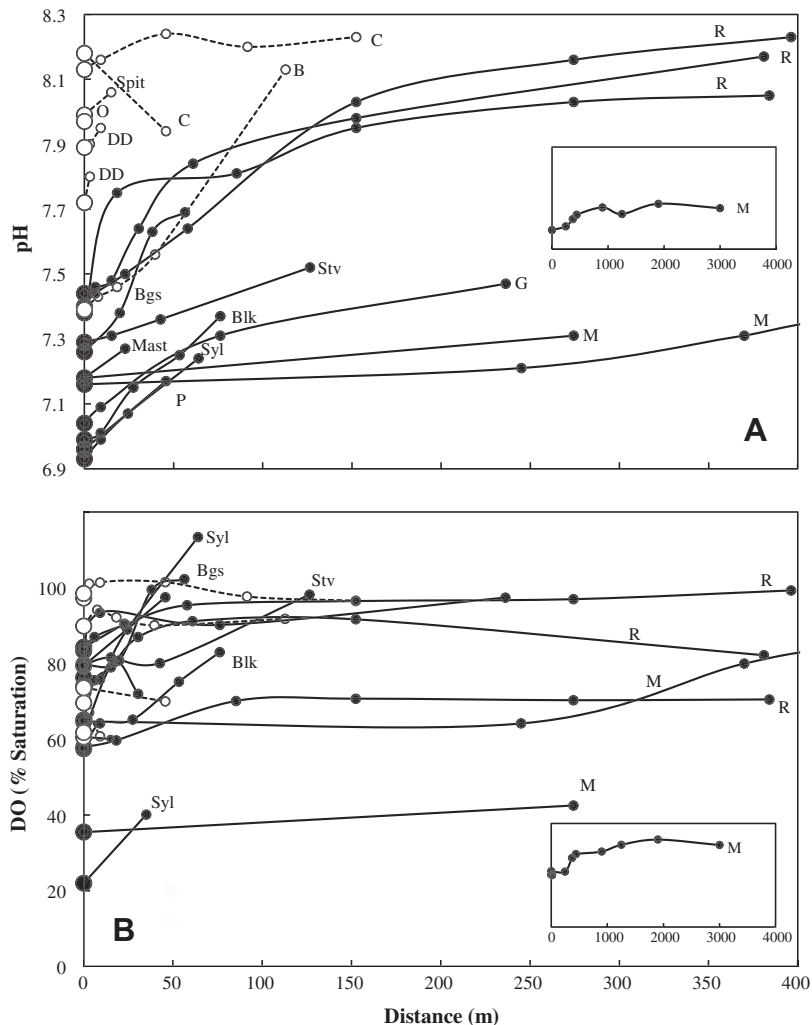


**Fig. 4.** Graphs of (A) pH and (B) DO (% saturation) measurements versus distance for phreatic springs and cave springs for traverses made in this study. Distances for one Maramec Spring (M) traverse are off-scale, but data are shown to scale in the inset. Symbols and labels as in Fig. 3.

Of the surface stream samples, two are undersaturated with respect to calcite. LaBarque Creek (Fig. 1) is undersaturated (Fig. 5) because its watershed is primarily underlain by St. Peter Sandstone, an extremely pure sandstone with >98% SiO<sub>2</sub> contents. Kiefer Creek (Fig. 1) was sampled during high flow conditions, dominated by event water that is typically undersaturated with respect to calcite (Fig. 5). Despite these exceptions, surface and cave waters in this region are almost always supersaturated with respect to calcite.

### 5.3. Total suspended solids and *E. coli*

Phreatic springs generally have lower *E. coli* levels than cave springs and surface streams due to reduction of suspended particles and less turbulent flow below the water table (Dussart-Baptista et al., 2003). Moreover, this study documents that the TSS in phreatic springs was half that of the cave springs and a quarter that of the surface streams (Table 1). Table 1 shows that the *E. coli* values for phreatic springs range from 6 cfu/100 mL to off-scale values (18% off-scale), while cave springs range from 15 cfu/100 mL to off-scale (25% off-scale). Excluding off-scale measurements, cave springs had average *E. coli* levels 100 cfu/100 mL higher than the phreatic springs. Bacterial levels are typically high after storms in

all samples, because turbulent flood waters have high suspended loads to which bacteria are adhered (Pronk et al., 2007).

### 5.4. Stable isotopes

Stable isotope data show that cave springs and surface streams have undergone more evaporation than phreatic springs (Fig. 6), but differences are small. Phreatic springs have an average  $\delta^{18}\text{O}$  value of  $-6.7\text{‰}$  and average  $\delta\text{D}$  value of  $-43\text{‰}$  (Table 1), which is close to the average value of local meteoric precipitation in St. Louis, Missouri (Winston and Criss, 2004). These similarities indicate that all these waters are derived from local meteoric precipitation that has become variably homogenized in shallow groundwater systems. It also suggests that these waters have a relatively long residence time within the aquifer according to a linear reservoir model, but residence times tend to be longer for the phreatic springs than for cave springs (Criss et al., 2007). An exception is Weldon Spring (Fig. 1), whose elevated average  $\delta^{18}\text{O}$  value of  $-5.5\text{‰}$  (Fig. 6) reflects the large contributions of evaporated lake water to its flow (Criss et al., 2001). In detail, the isotopic values of all these springs fluctuate seasonally, and are perturbed for several days following large rainfall events (Lakey and Krothe, 1996; Winston and Criss, 2004).

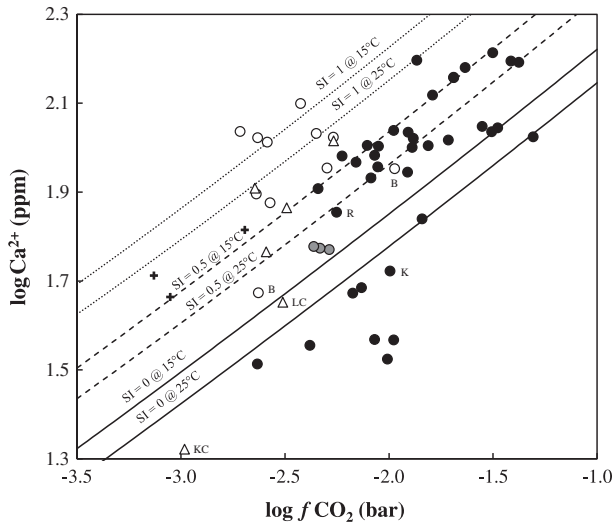


**Fig. 5.** The  $\log \text{Ca}^{2+}$  (mg/L) versus  $\log f \text{CO}_2$  (bar) for various water samples (symbols as in Fig. 1). Lines representing calcite SIs of 0.0 (solid line), 0.5 (dashed line), and 1.0 (dotted line) for temperatures of 15° and 25 °C are plotted for reference. Note that most cave springs and surface streams have SIs above 0.5 due to degassing of  $\text{CO}_2$  into the cave atmosphere; however, outliers exist, including Babler Cave Spring (B), Kiefer Creek (KC), and LaBarque Creek (LC). Atypical samples collected during a storm event for Kiefer Spring (K) and Rockwoods Spring (R) are also shown. Prairie Lake is off-scale with a  $\log \text{Ca}^{2+}$  (mg/L) of 0.98 and  $\log f \text{CO}_2$  (bar) of  $-5.35$ .

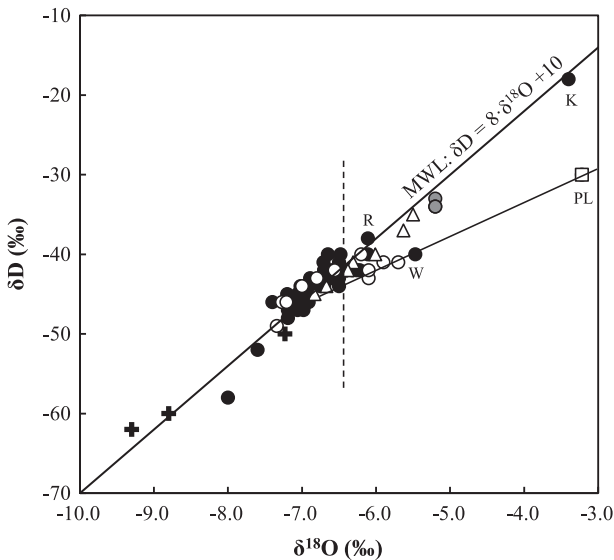


**Fig. 6.** Graph of  $\delta^{18}\text{O}$  (‰) and  $\delta\text{D}$  (‰) values for various water samples (symbols as in Fig. 1). Most phreatic springs lie on the global MWL with the exception of Weldon Spring (W), while many cave springs plot to the upper right of the main cluster of points indicating evaporative enrichment and isotopic exchange with the cave atmosphere, but differences are small. Prairie Lake (PL) shows the greatest enrichment, a common occurrence in lakes. An example evaporation trajectory from the average isotopic composition of meteoric precipitation (e.g.,  $-7.0$ ‰ and  $-46$ ‰ for  $\delta^{18}\text{O}$  and  $\delta\text{D}$ , respectively; see Winston and Criss, 2004) to Prairie Lake is shown on the diagram, and Weldon Spring lies directly on this trajectory. Note that most samples to the right of the dashed vertical reference line are surface streams, resurgences, or cave springs. Exceptions are the Kiefer Spring (K) and Rockwoods Spring (R) samples collected during a storm, demonstrating the variability of these features. WWTP waters (crosses) are isotopically depleted because the Missouri River is the dominant municipal water source.

The isotopic values of surface streams, on the other hand, are more variable and consistently higher than the values for springs ( $\delta^{18}\text{O} = -6.2$ ‰;  $\delta\text{D} = -41$ ‰; Table 1). This result is consistent with evaporative enrichment of  $^{18}\text{O}$  and D in surface and soil waters

during the summer and fall (Winston and Criss, 2004). The  $\delta^{18}\text{O}$  and  $\delta\text{D}$  values and their variability suggest that baseflow is dominated by meteoric water with a relatively short residence time (approximately 100 days).

Cave springs have intermediate average values ( $\delta^{18}\text{O} = -6.5$ ‰ and  $\delta\text{D} = -43$ ‰) and tend to have short residence times, which suggests that these systems include higher contributions of recent surface runoff than phreatic springs. Cave spring samples also are typically more evaporated as they, like most of the samples of surface streams, tend to plot to the upper right of the main cluster of points on Fig. 6. Under the high humidity environments typical of caves, evaporation and isotopic exchange can proceed and both  $\delta^{18}\text{O}$  and  $\delta\text{D}$  values of the water can increase significantly, but commonly without causing large displacement to the right of the MWL (e.g., Ingraham et al., 1990; also see Fig. 4.10 of Criss, 1999).

## 6. Discussion

The results show that DO and pH measurements of spring waters are helpful indicators of air-filled cave passages. Nevertheless, a number of complexities and special circumstance can influence the effectiveness of this geochemical method. Some caves may be geochemically detectable, but still completely inaccessible (too narrow, no entrance, etc.), while there may be large caves that can exist near phreatic springs.

The rate of interchange between the cave atmosphere and outside air is crucial to this method, because the  $\text{O}_2$  and  $\text{CO}_2$  contents of the cave air control the degassing and exchange processes of the water. The  $P_{\text{CO}_2}$  of cave air generally increases with increased distance into a cave (Baldini et al., 2006), though the rate at which the  $\text{CO}_2$ -rich cave air mixes with outside air depends on atmospheric conditions as well as on several other factors such as cave size, the size and number of cave entrances, and the number of through-going fractures (e.g., James, 2004; Herman, 2005). Steiner et al. (2007) found an increase in  $P_{\text{CO}_2}$  along traverses into several caves, with the highest values in the deepest parts of the cave during the summer months. However, the  $P_{\text{CO}_2}$  values vary seasonally, and Steiner et al. (2007) found that Cliff Cave air had homogeneous  $P_{\text{CO}_2}$  values during cold, winter conditions (see Fig. 1 for location).

In this study, the effect of the mixing rate of cave air and outside air was noted in the resurgence waters, whose DO and pH values were intermediate between those of phreatic springs and cave springs (Fig. 2). In the vadose caves above these resurgences, the  $P_{\text{CO}_2}$  likely increases and  $P_{\text{O}_2}$  decreases as the cave sump is approached. Further, the resurgence waters likely receive additional inputs of phreatic water before resurfacing, which is why they have an intermediate geochemical character.

Soil, epikarst, and aquifer properties also play an important role in determining the relative amounts of dissolved  $\text{O}_2$  and  $\text{CO}_2$ . The gas contents in the recharge waters depend on whether they percolated through soils rich in organic matter that enhance decomposition and create more anoxic conditions, or whether they traveled through bare rock fractures that have less organic matter and foster the retention of higher  $\text{O}_2$  and lower  $\text{CO}_2$  contents.

Additionally, the total organic C (TOC) in the recharge water may affect the  $\text{O}_2$  and  $\text{CO}_2$  contents of subsurface water if significant subsurface respiration occurs. Chemoorganoheterotrophic bacteria in the subsurface use TOC for a C and energy source (Chapelle, 2001; Pronk et al., 2006), and the degradation process would alter the DO and pH of these waters. Nevertheless, TOC concentrations can be affected by filtration in the soil by geochemical processes including adsorption–desorption, ion exchange, and trace metal interactions among others (Thurman, 1985).

Rivers and streams in the study area have the highest average TOC concentrations at 5.6 mg/L, cave springs have intermediate



values of 4.0 mg/L, and phreatic springs have the lowest concentrations at 2.7 mg/L (Davisson, written communication, 1998; Davisson, 2003). The differences in TOC between these waters may reflect their different residence times. If residence times are short, then the relatively slow bacterial reactions have insufficient time to alter the DO and pH of the water; despite this complication, residence times for phreatic springs tend to be rather long (Frederickson and Criss, 1999). Thus, phreatic waters are geochemically and biologically “filtered” of their TOC in the subsurface because they typically have slow flow paths. Conversely, cave springs and surface waters typically have faster flow paths and higher turbidity, resulting in higher TOC, DO, and pH. The distribution and reactivity of organic matter and other potential reductants in the aquifer can also have differential effects on O<sub>2</sub> and CO<sub>2</sub> concentrations. For example, potential redox materials such as MnO<sub>2</sub>, Fe(OH)<sub>3</sub>, Fe<sub>2</sub>O<sub>3</sub>, and sulfides in the aquifer can affect the DO contents.

Once the groundwater reaches the surface, the rate of aeration can exert significant control on the rate of gas equilibration. Thus, tufa deposits are commonly conspicuous immediately below orifices with rapids or waterfalls. Similarly, the discharge rate of the spring influences the rate of equilibration. For instance, Maramec Spring (Fig. 1), a first magnitude spring with an average discharge of 4.1 m<sup>3</sup>/s (Vineyard and Feder, 1982), requires significant time for the large water volume to equilibrate with air along the deep spring branch (see Fig. 4).

Further, the DO and pH along spring branches are simultaneously influenced by rates of photosynthesis and respiration. Photosynthetic activities during the hours of maximum solar radiation remove CO<sub>2</sub> and add O<sub>2</sub> to the spring waters, while respiration has the opposite effect and is the dominant biologic control on these dissolved gases during the night when photosynthetic organisms are inactive. Accordingly, diurnal DO and pH cycles have been noted (Parker et al., 2005; Hasenmueller, 2011) and, similarly, Rutherford and Hynes (1987) noted that diel fluctuations in the dissolved organic C (DOC) of stream water were consistent with daytime autochthonous production and nighttime uptake by heterotrophs. Moreover, Liu et al. (2007) found that these daily pH changes caused fluctuations in calcite and dolomite saturation. In this study, the highest DO was found in Sylvan Spring (Figs. 1 and 3), which had abundant aquatic vegetation and high nutrient concentrations.

## 7. Conclusions

Open cave passages are difficult to discover, but the orifices of carbonate-hosted springs are commonly conspicuous. The geochemical approach to cave discovery outlined here exploits the well understood changes in dissolved O<sub>2</sub> and CO<sub>2</sub> that occur when phreatic groundwaters encounter open air. It has been shown that cave springs have elevated DO and pH compared to phreatic springs, and that these cave spring systems have calcite SIs over 0.5. Cave spring waters are also typically higher in TSS and *E. coli* due to more turbulent flow in the subsurface, and they experience more isotopic enrichment than their phreatic spring counterparts. Once a karst spring has been located, DO and pH along with other conventional geochemical parameters can be used to detect open cave passages in the spring system.

## Acknowledgements

This work is part of the Ph.D. dissertation project of EAH at Washington University, and we gratefully acknowledge Washington University for supporting EAH under a Dissertation Fellowship. ICP-OES analyses were performed at the Nano Research Facility

(NRF), a member of the National Nanotechnology Infrastructure Network (NNIN), which is supported by the National Science Foundation under Grant No. ECS-0335765. Jeffrey Catalano, M. Lee Davisson, and William Winston provided valuable suggestions and discussion, and two anonymous reviewers gave helpful feedback. Kate Nelson, Yujie Xiong, Rachael Holley, and Heather Robinson are thanked for their assistance in data analysis and sample collection.

## References

- Back, W.B., Hanshaw, B.B., 1970. Comparison of chemical hydrogeology of the carbonate peninsulas of Florida and Yucatan. *J. Hydrol.* 10, 77–93.
- Baker, H., Streamer, P., 2002. Cave Maps of Missouri – Missouri River Region, MoDNR Division of Geology and Land Survey and Missouri Speleological Survey. <<http://www.missourigeologystore.com>>.
- Baldini, J.U.L., Baldini, L.M., McDermott, F., Clipson, N., 2006. Carbon dioxide sources, sinks, and spatial variability in shallow temperate zone caves: evidence from Ballynamintra Cave, Ireland. *J. Cave Karst Stud.* 68, 4–11.
- Baldini, J.U.L., McDermott, F., Hoffmann, D.L., Richards, D.A., Clipson, N., 2008. Very high-frequency and seasonal cave atmosphere PCO<sub>2</sub> variability: implications for stalagmite growth and oxygen isotope-based paleoclimate records. *Earth Planet. Sci. Lett.* 272, 118–129.
- Bechtel, T.D., Borsch, F.P., Gurk, M., 2007. Geophysical methods. In: Drew, D., Goldscheider, N. (Eds.), *Methods in Karst Hydrogeology*. Taylor & Francis, London, pp. 171–199.
- Boulding, J.R., Ginn, J.S., 2004. *Practical Handbook of Soil, Vadose Zone, and Groundwater Contamination: Assessment, Prevention, and Remediation*. Lewis Publishers, Florida.
- Brady, N.C., Weil, R.R., 2008. *The Nature and Properties of Soils*, 14th ed. Prentice Hall, Inc., Ohio.
- Brown, M.C., 1972. Karst hydrogeology and infrared imagery, an example. *Geol. Soc. Am. Bull.* 83, 3151–3154.
- Campbell, C., Latif, M., Foster, J., 1996. Application of thermography to karst hydrology. *J. Cave Karst Stud.* 58, 163–167.
- Chapelle, F.H., 2001. *Ground-water Microbiology and Geochemistry*. John Wiley & Sons, New York.
- Cook, J.C., 1965. Seismic imaging of underground cavities using reflection amplitude. *Geophysics* 30, 527–538.
- Criss, R.E., 1999. *Principles of Stable Isotope Distribution*. Oxford University Press, Oxford.
- Criss, R.E., Fernandes, S.A., Winston, W.E., 2001. Isotopic, geochemical and biological tracing of the source of an impacted karst spring, Weldon Spring, Missouri. *Environ. Forensics* 2, 99–103.
- Criss, R.E., Lippmann, J.L., Criss, E.M., Osburn, G.R., 2006. Caves of St. Louis County, Missouri. *Missouri Speleol.* 45, 1–18.
- Criss, R.E., Davisson, M.L., Surbeck, H., Winston, W.E., 2007. Isotopic techniques. In: Drew, D., Goldscheider, N. (Eds.), *Methods in Karst Hydrogeology*. Taylor & Francis, London, pp. 123–145.
- Criss, R.E., Osburn, G.R., House, R.S., 2009. The Ozark Plateaus: Missouri. In: Palmer, A.N., Palmer M.V. (Eds.), *Caves and Karst of the USA*. National Speleological Society, Huntsville, AL, pp. 156–170.
- Dandurand, J.L., Gout, R., Hoefs, J., Menschel, G., Schott, J., Usdowski, E., 1981. Kinetically controlled variations of major components and carbon and oxygen isotopes in a calcite-precipitating spring. *Chem. Geol.* 36, 299–315.
- Davisson, M.L., 1998. Written Communication: Lawrence Livermore National Laboratory, Lawrence Livermore National Laboratory, Livermore, California.
- Davisson, M.L., 2003. Organic matter in rivers: crossroads between climate and water quality. In: Criss, R.E., Wilson, D.A. (Eds.), *At the Confluence: Rivers, Floods, and Water Quality in the St. Louis Region*. MBG Press, St. Louis, pp. 161–178.
- Drever, J.I., 1997. *The Geochemistry of Natural Waters: Surface and Groundwater Environments*. Prentice-Hall, Upper Saddle River, New Jersey.
- Dreybrodt, W., 2005. Speleothem deposition. In: Culver, D.C., White, W.B. (Eds.), *Encyclopedia of Caves*. Elsevier Academic Press, New York, pp. 543–549.
- Dussart-Baptista, L., Massei, N., Dupont, J.-P., Jouenne, T., 2003. Transfer of bacteria-contaminated particles in a karst aquifer: evolution of contaminated materials from a sinkhole to a spring. *J. Hydrol.* 284, 285–295.
- Ek, C., Gewalt, M., 1985. Carbon-dioxide in cave atmospheres – new results from Belgium and comparison with some other countries. *Earth Surf. Process. Landforms* 10, 173–187.
- Fenneman, N.M., 1938. *Physiography of the Eastern United States*. McGraw-Hill, New York.
- Ford, D.C., 1971. Geologic structure and a new explanation of limestone cavern genesis. *Trans. Cave Res. Group Great Britain* 13, 81–94.
- Frederickson, G.C., Criss, R.E., 1999. Isotope hydrology and time constants of the unimpounded Meramec River basin, Missouri. *Chem. Geol.* 157, 303–317.
- Friedrich, A.J., Hasenmueller, E.A., Catalano, J.G., 2011. Composition and structure of nanocrystalline Fe and Mn oxide deposits: implications for contaminant mobility in a shallow karst system. *Chem. Geol.* 284, 82–96.
- Hach, 2005a. Method 8206, Chloride, Mercuric Nitrate, in Digital Titrator Model 16900 Manual. Hach Company.
- Hach, 2005b. Method 8038, Nitrogen, Ammonia: Nessler Method. Hach Company.



- Hach, 2005c. Method 10020, Nitrate: Chromotropic acid Method. Hach Company.
- Hach, 2005d. Method 8048, Phosphorus: Reactive (orthophosphate) Method. Hach Company.
- Hach, 2005e. Method 8190, Phosphorus: Total Digestion. Hach Company.
- Hasenmueller, E.A., 2011. The Hydrology and Geochemistry of Urban and Rural Watersheds in East-Central Missouri. Ph.D. Thesis, Washington Univ. in St. Louis, St. Louis, Missouri. <<http://openscholarship.wustl.edu/etd/585>>.
- Herman, J.S., 2005. Water chemistry in caves. In: Culver, D.C., White, W.B. (Eds.), *Encyclopedia of Caves*. Elsevier Academic Press, New York, pp. 609–614.
- Holland, H.D., Kirsipu, T., Huebner, J., Oxburgh, U., 1964. On some aspects of the chemical evolution of cave waters. *J. Geol.* 72, 36–67.
- Ingraham, N.L., Chapman, J.B., Hess, J.W., 1990. Stable isotopes in cave pool systems: Carlsbad Cavern, New Mexico, USA. *Chem. Geol.* 86, 65–74.
- Jacobson, R.L., Langmuir, D., 1974. Controls on the quality variations of some carbonate spring waters. *J. Hydrol.* 23, 247–265.
- James, J., 2004. Carbon dioxide-enriched cave air. In: Gunn, J. (Ed.), *Encyclopedia of Caves and Karst Science*. Fitzroy Dearborn, New York, pp. 183–184.
- Lakey, B., Krothe, N.C., 1996. Stable isotopic variation of storm discharge from a perennial karst spring, Indiana. *Water Resour. Res.* 32, 721–731.
- Lange, A.L., 1999. Geophysical studies at Kartchner Caverns State Park, Arizona. *J. Cave Karst Stud.* 61, 68–72.
- Langmuir, D., 1971. The geochemistry of some carbonate ground waters in central Pennsylvania. *Geochim. Cosmochim. Acta* 35, 1023–1045.
- Langmuir, D., 1997. *Aqueous Environmental Geochemistry*. Prentice-Hall, Upper Saddle River, New Jersey.
- Langmuir, D., Mahoney, J., 1985. Chemical equilibrium and kinetics of geochemical processes in ground water studies. In: Hitchon, B., Wallick, E.I. (Eds.), *Practical Applications of Ground Water Geochemistry*, Proc. 1st Canadian/American Conf. Hydrogeology. National Water Well Association, Worthington, Ohio, pp. 69–95.
- Liu, Z., Li, Q., Sun, H., Want, J., 2007. Seasonal, diurnal and storm-scale hydrochemical variations of typical epikarst springs in subtropical karst areas of SW China: soil CO<sub>2</sub> and dilution effects. *J. Hydrol.* 337, 207–223.
- MSDIS (Missouri Spatial Data Information Service. Data Resources), 2011. Missouri Spatial Data Information Service. University of Missouri. <<http://www.msdis.missouri.edu>>.
- Murphy, P.J., Parr, A., Strange, K., Hunter, G., Allshorn, S., Halliwell, R., Helm, J., Westerman, R., 2005. Investigating the nature and origins of Gapping Gill Main Chamber, North Yorkshire, UK, using ground penetrating radar and lidar. *Cave Karst Sci.* 32, 25–38.
- Noel, M., Xu, B., 1992. Cave detection using electrical resistivity tomography. *Cave Sci.* 19, 91–94.
- Omelon, C.R., Pollard, W.H., Andersen, D.T., 2006. A geochemical evaluation of perennial spring activity and associated mineral precipitates at Expedition Fjord, Axel Heiberg Island, Canadian High Arctic. *Appl. Geochem.* 21, 1–15.
- Palmer, A.N., 1975. The origin of maze caves. *Nat. Speleol. Soc. Bull.* 37, 56–76.
- Palmer, A.N., 2007. *Cave Geology*. Cave Books, Dayton, Ohio.
- Parker, S.R., Poulson, S.R., Gammons, C.H., DeGrandpre, M.D., 2005. Biogeochemical controls on diel cycling of stable isotopes of dissolved O<sub>2</sub> and dissolved inorganic carbon in the Big Hole River, Montana. *Environ. Sci. Technol.* 39, 7134–7140.
- Patrick Jr., W.H., 1977. Oxygen content of soil air by a field method. *Soil Sci. Soc. Am. J.* 41, 651–652.
- Pronk, M., Goldscheider, N., Zopfi, J., 2006. Monitoring of organic carbon, natural particles and bacteria in a deep karst system, Yverdon-les-Bains, Switzerland. In: Proc. 8th Conf. Limestone Hydrogeology, Neuchâtel (Switzerland), 21–23 September 2006, pp. 215–218.
- Pronk, M., Goldscheider, N., Zopfi, J., 2007. Particle-size distribution as indicator for fecal bacteria contamination of drinking water from karst springs. *Environ. Sci. Technol.* 41, 8400–8405.
- Rutherford, J.E., Hynes, H.B.N., 1987. Dissolved organic carbon in streams and groundwater. *Hydrobiologia* 154, 33–48.
- Smith, D.L., Smith, G.L., 1987. Use of vertical gravity gradient analyses to detect near-surface dissolution voids in karst terranes. In: Beck, B.F., Wilson, W.L. (Eds.), *Karst Hydrology: Engineering and Environmental Applications*. Balkema, Rotterdam, pp. 205–210.
- Steiner, A., Marlow, J., Orland, I., Wiseman, S., 2007. Unpublished Data: Department of Earth and Planetary Sciences. Washington University in St. Louis, St. Louis, Missouri.
- Stierman, D.J., 2004. Geophysical detection of caves and karstic voids. In: Gunn, J. (Ed.), *Encyclopedia of Caves and Karst Science*. Fitzroy Dearborn, New York, pp. 377–380.
- Thompson, J., Marvin, M., 2005. Experimental research on the use of thermography to locate heat signatures from caves. In: Proc. 17th National Cave and Karst Management Symp. National Speleological Society, Huntsville, Alabama, pp. 102–115.
- Thurman, E.M., 1985. *Organic Geochemistry of Natural Waters*. Martinus Nijhoff/Dr. W. Junk Publishers, Boston, Massachusetts.
- Troester, J.W., White, W.B., 1984. Seasonal fluctuations in the carbon dioxide partial pressure in a cave atmosphere. *Water Resour. Res.* 20, 153–156.
- Uzdowski, E., Hoefs, J., Menschel, G., 1979. Relationship between <sup>13</sup>C and <sup>18</sup>O fractionation and changes in major element composition in a recent calcite-depositing spring; a model of chemical variations with inorganic CaCO<sub>3</sub> precipitation. *Earth Planet. Sci. Lett.* 42, 267–276.
- USEPA (U.S. Environmental Protection Agency), 1971. Method 160.2: Residue, Non-filterable (Gravimetric, Dried at 103–105 C). U.S. Environmental Protection Agency.
- USEPA (U.S. Environmental Protection Agency), 1990. Method 200.7: Determinations of Metals and Trace Elements in Water and Wastes by Inductively Coupled Plasma-atomic Emission Spectrometry. U.S. Environmental Protection Agency, Revision 3.0.
- Vandike, J.E., 1995. *Surface Water Resources of Missouri* (Missouri State Water Plan Series – vol. 1). MoDNR Water Resour. Report 45.
- Vineyard, J., Feder, G.L., 1982. Springs of Missouri. MoDNR Water Resour. Report 29.
- White, W.B., 1988. *Geomorphology and Hydrology of Karst Terrains*. Oxford University Press, New York.
- White, W.B., 2005. Entrances. In: Culver, D.C., White, W.B. (Eds.), *Encyclopedia of Caves*. Elsevier Academic Press, New York, pp. 215–220.
- Winston, W.E., Criss, R.E., 2004. Dynamic hydrologic and geochemical response in a perennial karst spring. *Water Resour. Res.* 40, W05106.